



Monolayer-thick TiO precipitation in V-4Cr-4Ti alloy induced by proton irradiation

DOI:

[10.1016/j.scriptamat.2016.12.002](https://doi.org/10.1016/j.scriptamat.2016.12.002)

Document Version

Accepted author manuscript

[Link to publication record in Manchester Research Explorer](#)

Citation for published version (APA):

Impagnatiello, A., De Moraes Shubeita, S., Wady, P., Ipatova, I., Dawson, H., Barcellini, C., & Jimenez-Melero, E. (2017). Monolayer-thick TiO precipitation in V-4Cr-4Ti alloy induced by proton irradiation. *Scripta Materialia*, 130, 174–177. <https://doi.org/10.1016/j.scriptamat.2016.12.002>

Published in:

Scripta Materialia

Citing this paper

Please note that where the full-text provided on Manchester Research Explorer is the Author Accepted Manuscript or Proof version this may differ from the final Published version. If citing, it is advised that you check and use the publisher's definitive version.

General rights

Copyright and moral rights for the publications made accessible in the Research Explorer are retained by the authors and/or other copyright owners and it is a condition of accessing publications that users recognise and abide by the legal requirements associated with these rights.

Takedown policy

If you believe that this document breaches copyright please refer to the University of Manchester's Takedown Procedures [<http://man.ac.uk/04Y6Bo>] or contact openresearch@manchester.ac.uk providing relevant details, so we can investigate your claim.



Manuscript Number: SMM-16-1716R1

Title: Monolayer-thick TiO precipitation in V-4Cr-4Ti alloy induced by proton irradiation

Article Type: Regular article

Keywords: refractory metal;
precipitation;
lattice defects;
high-resolution electron microscopy;
nuclear fusion reactor.

Corresponding Author: Mr. Andrea Impagnatiello,

Corresponding Author's Institution: University of Manchester

First Author: Andrea Impagnatiello

Order of Authors: Andrea Impagnatiello; Samir M Shubeita; Paul T Wady; Iuliia Ipatova; Huw Dawson; Chiara Barcellini; Enrique Jimenez-Melero

Abstract: We have characterised to atomic resolution the mono-layer thick TiO-type precipitate induced by proton irradiation in V-4Cr-4Ti alloy at a dose of 0.3dpa and a temperature of 350°C. Its formation coincides with the coarsening radiation-induced interstitial $a/2\langle 111 \rangle$ dislocation loops that are already present at 300°C. The dislocation network induced by prior cold work is mostly recovered at 300°C and 0.3dpa, and is therefore expected to exert a minimal effect on the precipitate formation. This monolayer-thick precipitate constitutes an early stage in the radiation-induced aging process of V-4Cr-4Ti at low temperatures, and can potentially absorb additional light elements in reactor environments.

Moor Row, November 24, 2016

Dear Prof. Beyerlein,

Please find attached the resubmitted manuscript SMM-16-1716 entitled 'Monolayer-thick TiO precipitation in V-4Cr-4Ti alloy induced by proton irradiation' which has been significantly revised on the basis of the comments received by the reviewers.

The detailed response to the reviewers' comments, together with the revised version of the manuscript, is attached. We would like to thank the reviewers for their time and effort in appraising the manuscript. The comments received were pertinent and helpful in improving the manuscript. All the points raised have been addressed and the manuscript has been amended accordingly. We believe that the revisions made adequately address the points raised and should therefore present no further obstacle to publication.

Yours faithfully,

Andrea Impagnatiello

Mr. Andrea Impagnatiello
Dalton Cumbrian Facility, University of Manchester,
Westlakes Science & Technology Park, Moor Row, Cumbria, CA24 3HA, United Kingdom
Tel.: +44 (0)1946 508872, Email: andrea.impagnatiello@postgrad.manchester.ac.uk

Reply Referee report on Ms. No. SMM-16-1716 A. Impagnatiello et al.

We thank the reviewers for carefully reading the manuscript and the useful comments. We have addressed all those comments, which we feel have improved the article's quality.

Detailed response:

1.) *In figure 2, images for SA and SACW irradiated at 350C are necessary for better understanding of temperature effects.*

We have included additional text in the manuscript about the temperature effect. The novelty and impact of this work lies in the recovery of the CWed structure already at 300°C (Fig. 2) before the formation of monolayer-thick RIPs at 350°C (Fig. 3).

2.) *What is the relationship between the observed microstructure and the hardness? For example, for SA irradiated at 300C and 350C, where does the difference in hardening come?*

We have added some text to clarify the observed hardening behaviour at different temperatures in terms of the observed microstructure.

3.) *As the observed RIPs in this study is platelet, the description as "average size" may mislead.*

We have changed the average size of the monolayer-thick RIPs by their average length.

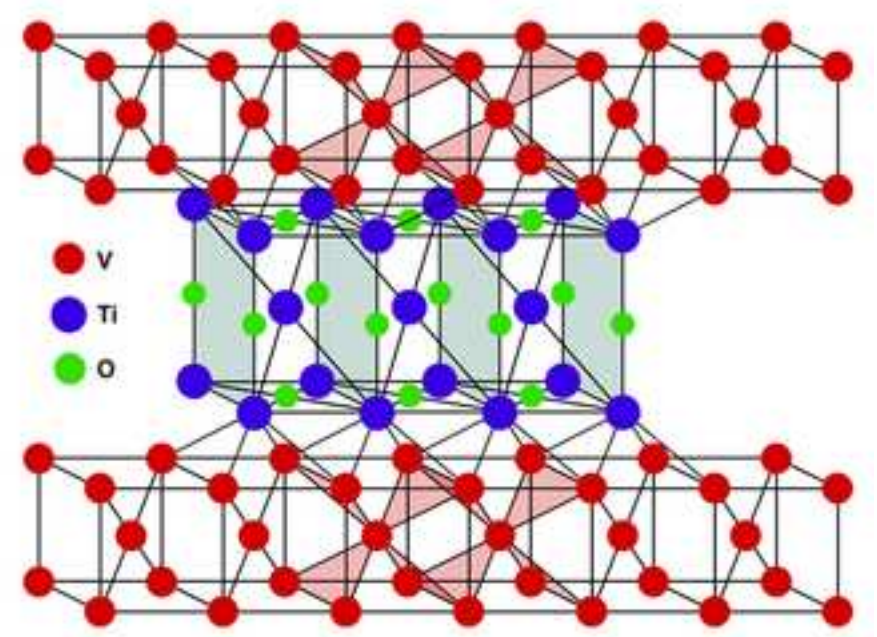
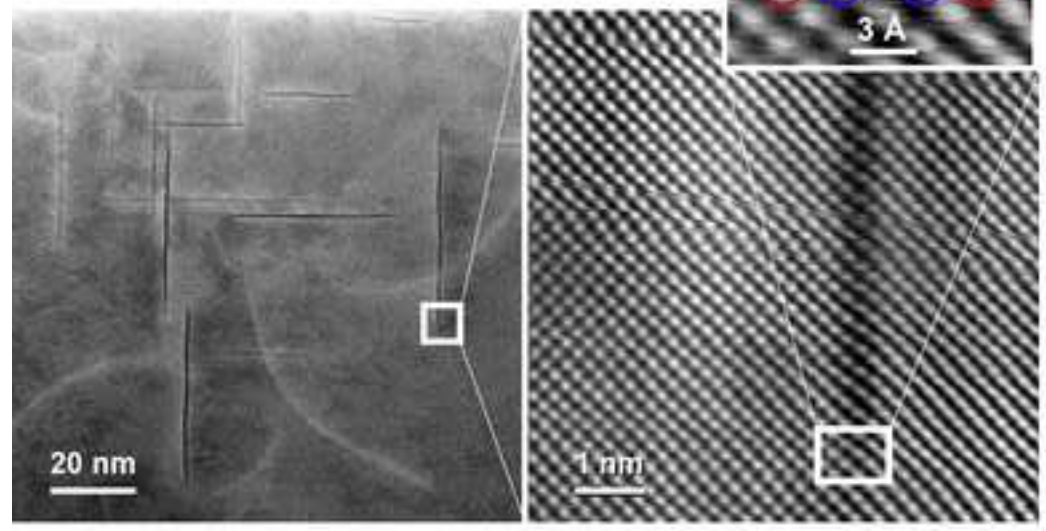
4.) *The description about recovery of the pre-existing dislocation network in SACW is contradicting in page 6 and page 7.*

We have clarified the contradiction in page 6 and 7.

5.) *Direct comparison with the results of neutron-irradiation might be difficult since the damage rate is exceedingly large.*

We have added some text about the difference in dose rate and particle fluence between neutron and proton irradiation. The formation and evolution of $a/2 \langle 111 \rangle$ unfaulted dislocation loops in our proton irradiated samples correspond to the observations reported in neutron-irradiated material. However the average loop size at 350°C in the proton irradiated samples (~85nm) is lower than the value reported in the literature for neutron irradiated samples, i.e. ~200nm (ref. 17), most likely due to the differences in damage dose rate.

V-4Cr-4Ti alloy
0.3 dpa, 350°C



1
2
3
4
5
6
7
8
9
10
11
12
13
14
15
16
17
18
19
20
21
22
23
24
25
26
27
28
29
30
31
32
33
34
35
36
37
38
39
40
41
42
43
44
45
46
47
48
49
50
51
52
53
54
55
56
57
58
59
60
61
62
63
64
65

Monolayer-thick TiO precipitation in V-4Cr-4Ti alloy induced by proton irradiation

A. Impagnatiello^{a,b,*}, S.M. Shubeita^b, P.T. Wady^b, I. Ipatova^{a,b}, H. Dawson^a, C. Barcellini^{a,b},
E. Jimenez-Melero^{a,b}

^a*School of Materials, The University of Manchester, Manchester M13 9PL, UK*

^b*Dalton Cumbrian Facility, The University of Manchester, Moor Row CA24 3HA, UK*

Corresponding author (*):

Dalton Cumbrian Facility

University of Manchester

Westlakes Science & Technology Park

Moor Row

CA24 3HA

United Kingdom

Tel.: +44 1946 508860

Email: andrea.impagnatiello@postgrad.manchester.ac.uk

Abstract

We have characterised to atomic resolution the mono-layer thick TiO-type precipitate induced by proton irradiation in V-4Cr-4Ti alloy at a dose of 0.3dpa and a temperature of 350°C. Its formation coincides with the coarsening radiation-induced interstitial $a/2\langle 111 \rangle$ dislocation loops that are already present at 300°C. The dislocation network induced by prior cold work is mostly recovered at 300°C and 0.3dpa, and is therefore expected to exert a minimal effect on the precipitate formation. This monolayer-thick precipitate constitutes an early stage in the radiation-induced aging process of V-4Cr-4Ti at low temperatures, and can potentially absorb additional light elements in reactor environments.

Keywords: refractory metal, precipitation, lattice defects, high-resolution electron microscopy, nuclear fusion reactor

1
2
3
4
5
6
7
8
9
10
11
12
13
14
15
16
17
18
19
20
21
22
23
24
25
26
27
28
29
30
31
32
33
Vanadium-based alloys currently constitute advanced candidate materials for the first wall of future fusion reactors such as DEMO [1, 2]. In particular, V-4Cr-4Ti alloy offers an outstanding combination of high-temperature strength and radiation resistance [3-5], coupled with low neutron activation [6, 7] and corrosion resistance to liquid metal coolants [8-10]. However, the presence of relatively small amounts of light atoms in the matrix can drastically increase the ductile-to-brittle transition temperature, and consequently also the minimum temperature for safe use of this alloy in structural components of the reactor [11, 12]. Ti acts as an effective scavenger for light elements by forming Ti(O,C,N) precipitates during the material's processing [13]. Cold working prior to annealing can be used to minimise the coarsening of the precipitates and increase the thermal creep resistance of the alloy [14]. Additionally, the interface of those nano-scale precipitates with the matrix can act as an effective sink for mobile lattice defects [15, 16]. Therefore, the radiation-induced hardening and embrittlement that take place in V-4Cr-4Ti below 400°C and at dose levels as low as 0.1-0.5dpa can be reduced.

34
35
36
37
38
39
40
41
42
43
44
45
46
47
48
49
50
51
52
53
54
55
56
57
58
59
60
61
62
63
64
65
Neutron irradiation of V-4Cr-4Ti alloy at temperatures below 275°C induces the formation of a high density of faulted dislocation loops with a Burgers vector of $a/2 \langle 110 \rangle$ and an average size of $\sim 3\text{nm}$. These small dislocation loops present a barrier strength lower than the Orowan value for impenetrable obstacles during dislocation gliding, and facilitate the formation of 50nm-wide cleared dislocation channels on $\{110\}$ slip planes at those low temperatures. This channel formation causes a pronounced loss of strain capability and uniform elongation in the V-4Cr-4Ti alloy. At higher neutron irradiation temperatures, $a/2 \langle 111 \rangle$ unfaulted dislocation loops predominate in the microstructure. They attain a larger average size of $\sim 200\text{nm}$, whereas their density is reduced to $< 10^{20}\text{m}^{-3}$ [17]. In parallel to the occurrence and evolution of dislocation loops with temperature, recent positron annihilation results revealed the presence of Ti-vacancy complexes in the vicinity of the

1 radiation-induced dislocation loops below 300°C [18]. These complexes may act as
2 precursors for the formation at higher temperatures of Ti-rich Radiation-Induced Precipitates
3 (RIPs). The growth of the additional precipitates induced by radiation may occur by changing
4 their morphology from sphere to platelet, and also the O/Ti ratio [19]. And enhanced V
5 content has also been reported in some of these RIPs [20]. Despite the key role of the RIPs in
6 improving the radiation resistance of V-4Cr-4Ti in the low temperature regime, a detailed
7 characterization of their structure and elemental content, especially at the interface with the
8 surrounding matrix, would allow the development of alloy microstructures with improved
9 radiation resistance. The potential effect of pre-existing dislocations due to prior cold
10 working on the precipitate formation should also be assessed. In this paper, we address these
11 points by using proton irradiation as a surrogate to neutron damage, in combination with
12 high-resolution electron microscopy to characterise both the RIPs and the presence of
13 dislocation structures in the matrix. This study provides a comparison of proton irradiated
14 microstructures with and without prior cold work. Generally speaking for other types of
15 materials, the presence of dislocations due to cold work would favourably increase radiation
16 resistance at relatively low dpa levels, since the dislocations would trap and slow down the
17 diffusion of radiation-induced point defects [21, 22]. Cold work can also be caused by the
18 manufacturing of the reactor components, so understanding the effect of cold work on
19 materials that will be under irradiation becomes even more important.

20
21
22
23
24
25
26
27
28
29
30
31
32
33
34
35
36
37
38
39
40
41
42
43
44
45
46 Equivalent V-4Cr-4Ti (wt.%) samples were solution-annealed (SA) at 1100°C for
47 2 hours and afterwards water quenched to room temperature. Some of the material was
48 subsequently 10% cold rolled (SACW). The sample surface was ground to 4000 grit SiC
49 paper, and then electro-polished using an electrolyte of 60vol.% methanol – 35vol.%
50 2-buthoxyethanol – 5vol.% perchloric acid (60%) at a temperature of -35°C. After that, the
51 samples were irradiated with a 1.4MeV proton beam produced using the 5MV tandem ion
52
53
54
55
56
57
58
59
60
61
62
63
64
65

1
2
3
4
5
6
7
8
9
10
11
12
13
14
15
16
17
18
19
20
21
22
23
24
25
26
27
28
29
30
31
32
33
34
35
36
37
38
39
40
41
42
43
44
45
46
47
48
49
50
51
52
53
54
55
56
57
58
59
60
61
62
63
64
65

accelerator of the Dalton Cumbrian Facility [23]. The beam current deposited on the samples was $\sim 28\mu\text{A}$, and the damage rate was $3\times 10^{-6}\text{dpa/s}$. We achieved a particle flux of $\sim 8.7\times 10^{17}\text{ protons/m}^2\text{s}$. The value of proton fluence of $\sim 8 \times 10^{22}\text{ particles/cm}^2$ is close to the fluence of $\sim 10^{24}\text{ neutrons/cm}^2$ from previous neutron irradiations of V-4Cr-4Ti samples [17].

The temperature during irradiation (either 300 or 350°C) was monitored both with welded thermocouples on the sample surface adjacent to the irradiated area, and also with a non-contact pyrometer. For transmission electron microscope (TEM) imaging and analysis, discs were prepared by mechanical pre-thinning, followed by electro-polishing using the same electrolyte and temperature as previously mentioned. In order to characterise the damaged structure, we used a FEI Tecnai T20 with LaB_6 crystal and an FEI Titan G2 80-200 aberration-corrected S/TEM with an X-FEG and ChemiSTEMTM technology [24], both microscopes operating at 200kV. The thickness of the disc area studied by TEM was derived from the fringes spacing of the convergent beam electron diffraction pattern, the interstitial or vacancy nature of the defects using the inside-outside method, and the Burgers vector from the $\mathbf{g}\cdot\mathbf{b}=0$ invisibility criterion [25, 26]. Vickers hardness measurements were taken using a load of 0.025g, resulting in an indentation depth of $\sim 8\mu\text{m}$, which is close to the 60% of the Bragg peak position from the irradiated sample surface.

The initial (SA) microstructure contained a fine dispersion of plate-like Ti(O,C,N) precipitates [27], together with a number of cuboidal Ti-rich precipitates decorating the grain boundaries of the matrix. Fig. 1a shows a scanning electron micrograph of the cross section of the SA sample surface irradiated at 350°C. The large plate-like precipitates formed during prior annealing treatment are clearly visible in the image. A relatively bright line at $\sim 15\mu\text{m}$ below the sample surface can be observed passing through two neighbouring grains of the matrix. The position of this bright line agrees well with the Bragg peak position of $14\mu\text{m}$ calculated using the SRIM software [28], see Fig. 1b. In the region of the Bragg peak, the

1 lattice is mostly damaged, the channelling of electrons is more impeded and therefore the
2 BSE signal increases. We have prepared TEM discs of the irradiated samples at a depth of
3
4 60% of the Bragg peak position from the sample surface. This corresponded approximately to
5
6 an 8 μ m depth from the surface and a damage dose of 0.3dpa in the studied samples.
7
8

9
10 Fig. 2 shows the TEM images of the SA and SACW samples, both before and after
11 having been irradiated up to 0.3dpa at a constant temperature of 300°C. Before irradiation
12 and cold work, the prior annealing at 1100°C led to a microstructure free from the dislocation
13 networks and other defects that are instead present after 10% cold work. After irradiation,
14 dislocation loops are present in the SA sample with a density of $\sim 11 \times 10^{21} \text{m}^{-3}$. The majority of
15 these loops have a Burgers vector of $a/2 \langle 111 \rangle$ and their average size is 12nm. A slightly
16 lower density of dislocation loops is present in the SACW sample after irradiation, namely
17 $\sim 9 \times 10^{21} \text{m}^{-3}$, and their average diameter of 14 nm is close to the value for the SA sample. It is
18 remarkable that the pre-existing dislocation network in the SACW sample is mostly
19 recovered after irradiation.
20
21
22
23
24
25
26
27
28
29
30
31
32
33

34 The damaged microstructure of the SA sample after irradiation up to 0.3dpa at 350°C
35 is shown in Fig. 3a. Interstitial $a/2 \langle 111 \rangle$ dislocation loops are also present in the
36 microstructure. They are characterised by a larger average diameter of 86 nm and a lower
37 density of $\sim 2 \times 10^{21} \text{m}^{-3}$, as compared to the dislocation loops observed at 300°C. However, at
38 350°C we also observed new plate-shaped RIPs, oriented along the $\{100\}$ planes of the
39 V matrix. They appear with an [average length](#) of 56nm and a density of $\sim 1.5 \times 10^{21} \text{m}^{-3}$. Fig. 3b
40 and c show a higher-resolution image of the RIPs. The precipitates seem to be composed of
41 only one atomic layer. Chemical analysis using energy-dispersive spectroscopy confirmed the
42 presence of Ti [27]. These results suggest that these observed RIPs correspond to TiO-type
43 precipitates with a lattice parameter of 0.42nm [29] and the Baker–Nutting orientation
44 relationship with the matrix [30]: $[001]_{\text{TiO}} // [001]_{\text{V}}$, $(110)_{\text{TiO}} // (100)_{\text{V}}$. This assumption
45
46
47
48
49
50
51
52
53
54
55
56
57
58
59
60
61
62
63
64
65

1 allows us to propose in Fig. 3e-f a crystal model of the plate-like precipitates that is
2 consistent with the atomic resolution TEM data of Fig.3c-e.
3

4
5 Table 1 summarises the microstructure of the irradiated samples in terms of average
6
7 length and density of RIPs and dislocation loops, together with the change in hardness due to
8
9 irradiation. The number of dislocation loops in the SACW sample is somewhat lower than in
10
11 the SA at 300°C. The presence of the dislocation network in the SACW sample may have
12
13 reduced the mobility of the radiation-induced point defects that eventually form dislocation
14
15 loops. As reported for cold-worked irradiated steels, a significant reduction of the initial
16
17 dislocation network is required for the development of observable dislocation loops [31].
18
19 Irradiation at intermediate doses would be required to understand the evolution of pre-
20
21 existent dislocations to achieve their full recovery at the relatively low temperature of 300°C.
22
23 In this alloy recovery occurs during annealing above 400°C in the absence of irradiation [32].
24
25 Furthermore, the hardness values of the SA and SACW samples after irradiation at 300°C lie
26
27 very close. This is due to their dislocation structures after irradiation being also very similar.
28
29 Taking into account that the cold work raised the hardness of the material before irradiation,
30
31 the hardness change after irradiation seems to decrease with the amount of cold work prior
32
33 irradiation. In conclusion it appears that the initial 10% cold work does not affect
34
35 significantly the final hardness of the alloy after irradiation.
36
37
38
39
40
41
42
43

44 Dislocation loops found in all the irradiated samples were of interstitial nature,
45
46 consistent with previous work on neutron irradiated V-4Cr-4Ti in this temperature range [17].
47
48 They are unfaulted and the predominant Burgers vector is $a/2 \langle 111 \rangle$. Faulted dislocation
49
50 loops with a Burgers vector of $a/2 \langle 110 \rangle$ were reported for temperatures below 300°C in
51
52 previous neutron-irradiation studies [17]. Molecular dynamic simulations previously showed
53
54 that this latter type of dislocation loop has a relatively high formation energy and become
55
56 unstable at high temperatures [33]. We found that the increase in irradiation temperature from
57
58
59
60
61
62
63
64
65

1 300°C to 350°C causes a reduction in the density of dislocation loops and an increase in the
2 average size of the loops. As a consequence, the irradiation-induced hardening of the alloy
3
4 (ΔHV_{irr}) diminishes with increasing temperature above 300°C, see Table 1. A higher density
5
6 of finer loops at 300°C implies more obstacles to the motion of dislocations and, as a
7
8 consequence, an enhanced irradiation hardening [34]. The decrease in hardening due to the
9
10 temperature evolution of the dislocation structure is partially compensated by the appearance
11
12 of RIPs at 350°C [35]. Differences in dose rate between neutron and proton irradiation are
13
14 expected to yield a lower average loop size in the proton irradiated specimens (~85nm) as
15
16 compared to neutron irradiation (~200nm) [36].
17
18
19
20
21

22 The appearance of Ti-rich RIPs at a radiation dose of 0.3dpa occurred between 300°C
23
24 and 350°C, in agreement with previous neutron irradiation experiments [18]. In non-
25
26 irradiated conditions, the formation plate-like Ti(O,C,N) precipitates is induced above 500°C
27
28 by climbing dislocations during recovery [37]. Proton irradiation at lower temperatures has
29
30 triggered the formation of dislocation loops, and at 350°C also the formation of additional
31
32 plate-like TiO-type precipitates. The radiation-induced mobile vacancies would increase the
33
34 diffusion of substitutional Ti atoms, and the occurrence of Ti-vacancy complexes close to the
35
36 dislocation loops, where the additional TiO-type precipitates form [17, 18]. The crystal
37
38 structure model in Fig. 3e describes the precipitate platelet as an fcc TiO monolayer, whose
39
40 interface with the V matrix is coherent along the sides of the platelet. This monolayer platelet
41
42 could evidence that the proposed Ti spherical clusters [19] evolve to a platelet Guinier-
43
44 Preston (GP) zone visible with TEM techniques. The GP zone would finally evolve to a
45
46 thicker plate as the dose is increased. The thickness of these TiO-type plates has been
47
48 reported to be ~1-3nm at a neutron radiation dose of 4dpa and a temperature of ~510°C [38].
49
50 This precipitation sequence is similar to the precipitation behaviour observed in Al-Cu alloys
51
52 during annealing at 130°C, where monolayer, bilayer and multilayer Cu-rich plate-like
53
54
55
56
57
58
59
60
61
62
63
64
65

1 precipitates correspond to different stages of hardening during aging [39]. Therefore, the
2 initial Ti-vacancy clusters, the monolayer platelet reported in this work, and the multilayer
3 TiO-type precipitates characterize different stages of radiation-induced precipitation
4 hardening in the V-4Cr-4Ti alloy.
5
6
7

8
9 In conclusion, our results on proton-irradiated V-4Cr-4Ti alloy lie in accordance with the
10 nature and evolution of dislocation loops observed in the same alloy irradiated with neutrons
11 at equivalent temperatures. Our TEM data also revealed that the dislocation networks induced
12 by prior cold work are mainly recovered at 300°C and a radiation dose of 0.3dpa. Therefore
13 those pre-existing dislocations exert a minor effect on the formation of radiation-induced
14 TiO-type plate precipitates observed at 350°C. Our high-resolution TEM data allowed us to
15 characterise the monolayer-thick TiO precipitate. This precipitate constitutes an early stage in
16 the radiation-induced aging process of V-4Cr-4Ti at relatively low temperatures, and
17 therefore possesses the capacity of absorbing additional light elements in fusion reactor
18 operation conditions.
19
20
21

22 We acknowledge the Engineering and Physical Sciences Research Council (EPSRC) for
23 providing funding for this project via the Centre for Doctoral Training in the Science and
24 Technology of Fusion Energy (<http://www.fusion-cdt.ac.uk/>). The work described was
25 supported in part by the Dalton Cumbrian Facility Project, a joint initiative of The University
26 of Manchester and the Nuclear Decommissioning Authority. We would also like to thank
27 A.D. Smith and N. Mason for their assistance during the irradiation experiment.
28
29
30
31
32
33

34 **References**

- 35 [1] J.M. Chen, V.M. Chernov, R.J. Kurtz, T. Muroga. J. Nucl. Mater. 417 (2011) 289.
36 [2] T. Muroga, J.M. Chen, V.M. Chernov, R.J. Kurtz, M. Le Flem. J. Nucl. Mater. 455 (2014)
37 263.
38 [3] K. Fukumoto, T. Morimura, T. Tanaka, A. Kimura, K. Abe, H. Takahashi, et al. J. Nucl.
39 Mater. 239 (1996) 170.
40
41
42
43
44
45
46
47
48
49
50
51
52
53
54
55
56
57
58
59
60
61
62
63
64
65

- 1
2
3
4
5
6
7
8
9
10
11
12
13
14
15
16
17
18
19
20
21
22
23
24
25
26
27
28
29
30
31
32
33
34
35
36
37
38
39
40
41
42
43
44
45
46
47
48
49
50
51
52
53
54
55
56
57
58
59
60
61
62
63
64
65
- [4] T. Muroga, J.M. Chen, V.M. Chernov, K. Fukumoto, D.T. Hoelzer, R.J. Kurtz, et al. J. Nucl. Mater. 367-370 (2007) 780.
- [5] F.A. Garner, T. Okita, N. Sekimura. J. Nucl. Mater. 417 (2011) 314.
- [6] D.L. Smith, M.C. Billone, K. Natesan. Int. J. Refract. Met. Hard Mat. 18 (2000) 213.
- [7] D.V. Markovskij. Fusion Eng. Des. 51-52 (2000) 695.
- [8] R. L. Ammon. Int. Met. Rev. 5 (1980) 255.
- [9] B.A. Pint, J.L. Moser, P.F. Tortorelli. Fusion Eng. Des. 81 (2006) 901.
- [10] I.V. Borovitskaya, I.E. Lyublinski, V.V. Paramonova, S.N. Korshunov, A.N. Mansurova, M.M. Lyakhovitskiy, et al. Inorg. Mater. Appl. Res. 6 (2015) 133.
- [11] S.J. Zinkle, N.M. Ghoniem, Fusion Eng. Des. 51-52 (2000) 55.
- [12] A.-A. Tavassoli. J. Nucl. Mater. 302 (2002) 73.
- [13] D.R. Diercks, B.A. Loomis, J. Nucl. Mater. 141-143 (1986) 1117.
- [14] T. Muroga, T. Nagasaka, P.F. Zheng, J.M. Chen, Adv. Sci. Technol. 73 (2010) 22.
- [15] M.S. Staltsov, I.I. Chernov, B.A. Kalin, K.Z. Oo, A.A. Polyansky, O.S. Staltsova, et al., J. Nucl. Mater. 461 (2015) 56.
- [16] A. van Veen, A.V. Fedorov, A.I. Ryazanov, J. Nucl. Mater. 258-263 (1998) 1400.
- [17] P.M. Rice, S.J. Zinkle. J. Nucl. Mater. 258-263 (1998) 1414.
- [18] K.-i. Fukumoto, H. Matsui, H. Ohkubo, Z. Tang, Y. Nagai, M. Hasegawa. J. Nucl. Mater. 373 (2008) 289.
- [19] N. Nita, Y. Anma, H. Matsui, T. Ohkubo, K. Hono. J. Nucl. Mater. 367 (2007) 858.
- [20] M. Hatakeyama, T. Nagasaka, T. Muroga, T. Toyama, I. Yamagata. J. Nucl. Mater. 442 (2013) S346.
- [21] S.J. Zinkle, L.L. Snead. Annu. Rev. Mater. Res. 44 (2014) 241.
- [22] J.O. Stiegler, E.E. Bloom. J. Nucl. Mater. 41 (1971) 341.

- 1
2
3
4
5
6
7
8
9
10
11
12
13
14
15
16
17
18
19
20
21
22
23
24
25
26
27
28
29
30
31
32
33
34
35
36
37
38
39
40
41
42
43
44
45
46
47
48
49
50
51
52
53
54
55
56
57
58
59
60
61
62
63
64
65
- [23] P.T. Wady, A. Draude, S.M. Shubeita, A.D. Smith, N. Mason, S.M. Pimblott, et al. Nucl. Instr. Meth. Phys. Res. A 806 (2016) 109.
- [24] D. Sudfeld, O. Lourie, S. Kujawa. J. Phys.: Conf. Series 522 (2014) 012026.
- [25] S.M. Allen. Philos. Mag. A 43 (1981) 325.
- [26] M.L. Jenkins, M.A. Kirk. Characterization of Radiation Damage by Transmission Electron Microscopy, Institute of Physics Publishing, 2001.
- [27] A. Impagnatiello, D. Hernandez-Maldonado, G. Bertali, E. Prestat, D. Kepaptsoglou, Q. Ramasse, et al. Scripta Mater. 126 (2017) 50.
- [28] J.F. Ziegler, M.D. Ziegler, J.P. Biersack. Nucl. Instrum. Meth. B 268 (2010) 1818.
- [29] K.H. Kramer. J. Less-Common Met. 21 (1970) 365.
- [30] J.W. Edington. Practical Electron Microscopy in Materials Science, Gloeilampenfabrieken, Eindhoven, 1975.
- [31] S.J. Zinkle, P.J. Maziasz, R.E. Stoller. J. Nucl. Mater. 206 (1993) 266.
- [32] A.N. Gubbi, A.F. Rowcliffe. J. Nucl. Mater. 233 (1996) 497.
- [33] L.A Zepeda-Ruiz, J. Marian, B.D. Wirth. Philos. Mag. 85 (2005) 697.
- [34] K.-i. Fukumoto, H. Matsui, H. Tsai, D.L. Smith. J. Nucl. Mater. 283 (2000) 492.
- [35] K.-i. Fukumoto, H. Matsui, Y. Candra, K. Takahashi, H. Sasanuma, S. Nagata, et al. J. Nucl. Mater. 283 (2000) 535.
- [36] C. Abromeit. J. Nucl. Mater. 216 (1994) 78.
- [37] T. Leguey, R. Pareja. J. Nucl. Mater. 279 (2000) 216.
- [38] D.T. Hoelzer, S.J. Zinkle, DOE/ER-0313/29 (2000) 19.
- [39] S.K. Son, M. Takeda, M. Mitome, Y. Bando, T. Endo. Mater. Lett. 59 (2005) 629.
- [40] ASTM E521-96, Standard Practice for Neutron Radiation Damage Simulation by Charged-Particle Irradiation, 2009.

Table 1. Average length/size and density of the dislocation loops and irradiation-induced Ti-rich precipitates observed in the irradiated V-4Cr-4Ti samples. together with the initial hardness value (HV_i) and the change in hardness due to proton irradiation (ΔHV_{irr}).

sample condition	HV_i	$T_{irr}(^{\circ}C)$	dose (dpa)	ΔHV_{irr}	Dislocation loops		Irr. induced Precipitates	
					average size(nm)	density x $10^{21}m^{-3}$	average length(nm)	density x $10^{21}m^{-3}$
SA	196±8	300	0.3	130±19	12	11	-	-
	196±8	350	0.3	90±18	85	2	56	1.5
SA + 10%CW	217±13	300	0.3	104±26	14	9	-	-

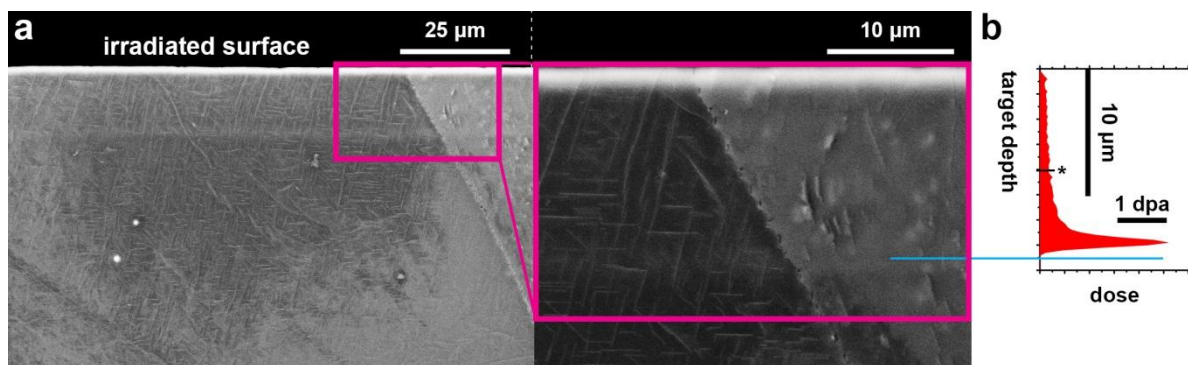


Fig. 1. (a) SEM (BSE, 30keV) image of the cross section of the solution-annealed V-4Cr-4Ti alloy irradiated up to 0.3dpa at 350°C, and (b) simulated damage profile using the SRIM software with the quick Kinchin – Pease approach [40] and the total current deposited on the sample during the irradiation experiment. The asterisk locates the depth equal to 60% the Bragg peak position, and denotes the region in the sample from where TEM foils were prepared.

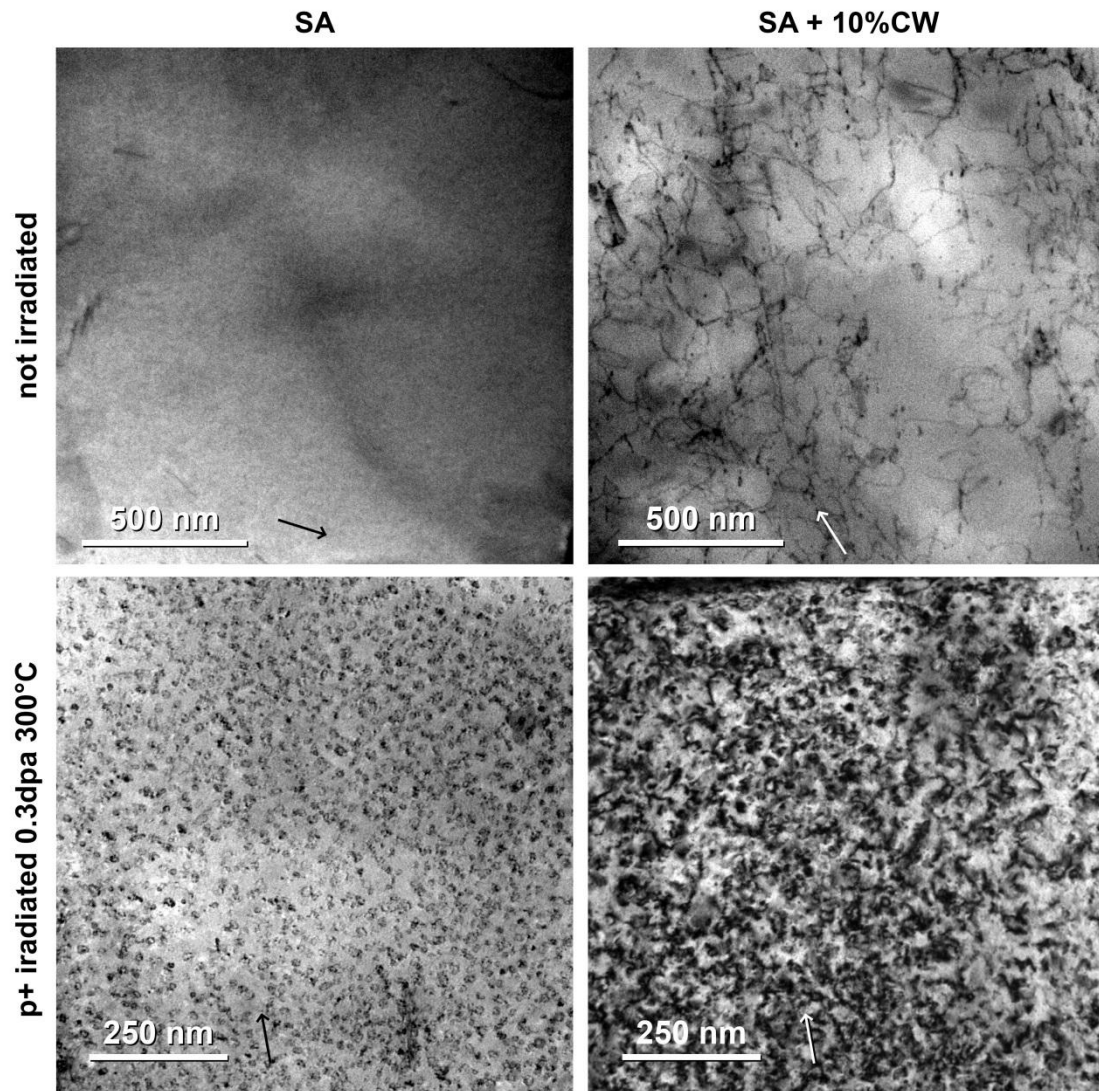


Fig. 2. TEM images of the microstructure of the solution annealed (SA) and SA+10% cold worked (CW) samples, before and after proton irradiation up to 0.3dpa at 300°C. The arrows show the g 200 direction.

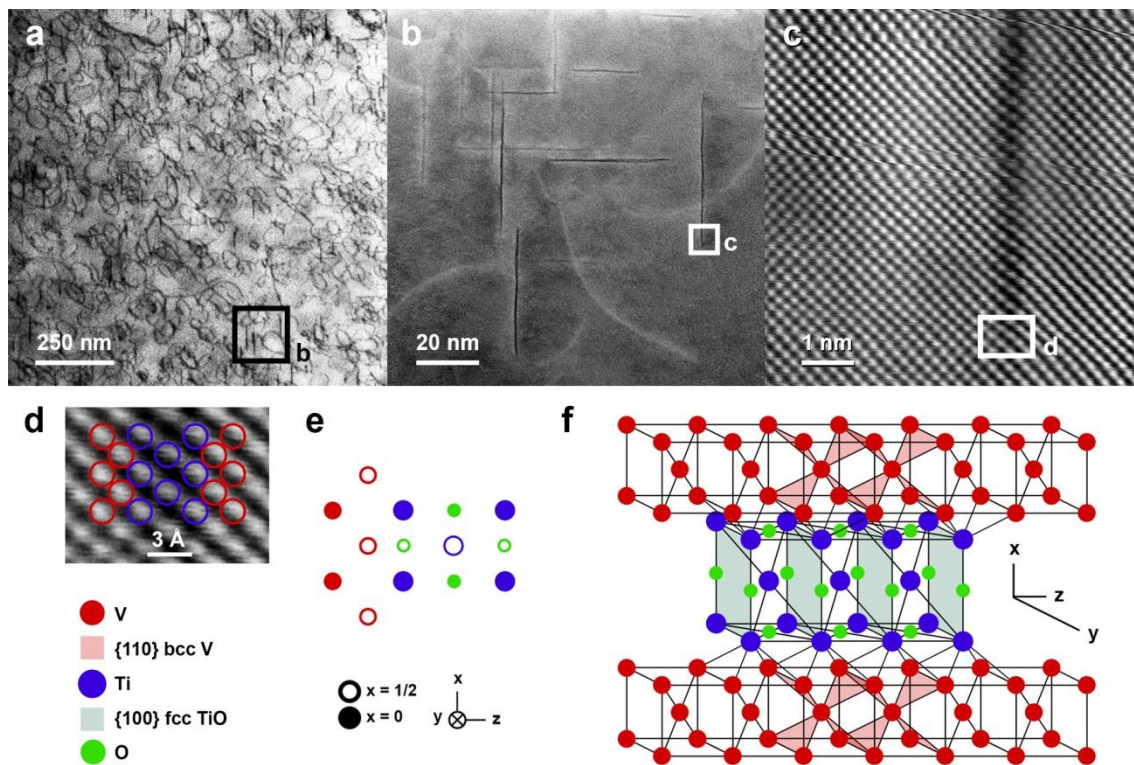


Fig. 3. (a) Microstructure of the solution-annealed sample after undergoing proton irradiation up to 0.3dpa at 350°C, (b) detail from (a) of Ti-rich radiation induced precipitates aligned along the [100] direction of the vanadium matrix, together with a number of dislocation loops, (c) atomic-resolution image of the region outlined by the square in (b), (d) atomic-resolution detail of the region outlined by the square in (c) where the position of the Ti and V atoms are indicated by blue and red circles, respectively, (e) upper and (f) 3-D view of the crystal structure model of the plate-like precipitate shown in (c) and (d). (a) was obtained in TEM mode, whereas the (b-d) were collected in STEM mode. In all images, $\mathbf{B} = [001]$ and $\mathbf{g} 200$ lies parallel to the scale bar.